

A GABAergic nigrotectal pathway for coordination of drinking behavior

Mark A Rossi¹, Haofang E Li¹, Dongye Lu¹, Il Hwan Kim², Ryan A Bartholomew¹, Erin Gaidis¹, Joseph W Barter^{1,3}, Namsoo Kim¹, Min Tong Cai¹, Scott H Soderling^{2,4} & Henry H Yin^{1,3,4}

The contribution of basal ganglia outputs to consummatory behavior remains poorly understood. We recorded from the substantia nigra pars reticulata (SNR), the major basal ganglia output nucleus, during self-initiated drinking in mice. The firing rates of many lateral SNR neurons were time-locked to individual licks. These neurons send GABAergic projections to the deep layers of the orofacial region of the lateral tectum (superior colliculus, SC). Many tectal neurons were also time-locked to licking, but their activity was usually in antiphase with that of SNR neurons, suggesting inhibitory nigrotectal projections. We used optogenetics to selectively activate the GABAergic nigrotectal afferents in the deep layers of the SC. Photo-stimulation of the nigrotectal projections transiently inhibited the activity of the lick-related tectal neurons, disrupted their licking-related oscillatory pattern and suppressed self-initiated drinking. These results demonstrate that GABAergic nigrotectal projections have a crucial role in coordinating drinking behavior.

Consummatory behaviors such as eating and drinking are critical for survival and energy homeostasis^{1,2}. They require patterned orofacial movements with cyclic coordination of many muscles. In rodents and many other species, drinking is achieved by stereotyped and repetitive licking movements with a relatively constant frequency. Although the organization of the brainstem nuclei involved in mastication and licking is well characterized³, it remains unclear how these nuclei are influenced by descending commands from the brain.

A major source of descending signals is the basal ganglia, a large set of subcortical nuclei implicated in voluntary behavior. Anatomically, the basal ganglia output from the SNR can influence the activity of central pattern generators in the medullary reticular formation via their projections to the tectum. By common consensus, there are multiple parallel basal ganglia networks with functional specialization^{4–6}, and their outputs reach areas such as the thalamus, tectum and reticular formation^{7,8}. Lesion and inactivation studies have suggested that the nigrotectal projections are important for orofacial behaviors^{9–11}. Intranigral injections of muscimol (GABA-A agonist) produce oral stereotypy that can be abolished by electrolytic lesions of the SC⁹. However, the function of the nigrotectal projections in voluntary orofacial behavior remains poorly understood.

Although recent studies have shown that descending motor cortical projections can influence licking in adult mice¹², self-initiated licking is preserved in cats that lack only the cerebral cortex¹³, suggesting a key role for other structures such as the basal ganglia. Indeed, without intact basal ganglia, cats and rats cannot lick for milk and water even though they are able to orient their heads and move toward auditory, olfactory and tactile stimuli. These animals only show ‘reflexive’

licking and chewing when food or milk is placed into contact with their lips^{14,15}.

To study how basal ganglia output can regulate consummatory behavior, we combined single-unit recording and optogenetics in mice to examine the role of the GABAergic SNR output neurons and their targets in the SC in drinking behavior. We found that the nigrotectal projections are critical for coordinating self-initiated licking movements.

RESULTS

We recorded single-unit activity from the SNR or the lateral SC as freely behaving mice voluntarily consumed sucrose solution from a drinking spout (**Supplementary Fig. 1a–d**). Individual spout contacts were recorded with a contact lickometer¹⁶. In agreement with previous work, voluntary licking in mice was highly stereotyped, consisting of bouts of rhythmic protrusions and retractions of the tongue at a relatively fixed rate (6–9 Hz). We found that mice licked in frequent bouts, and the frequency of licking was consistent within bouts^{1,17,18}.

During consummatory licking, the mouse’s tongue exhibits rhythmic, stereotyped oscillations of protrusions and retractions¹⁸. This rhythmic orofacial movement was reflected in the firing rates of neurons in the SNR and the SC (**Figs. 1 and 2**). Many SNR neurons showed activity that peaked at the time the tongue contacted the spout and was tightly coupled with rhythmic licking (**Fig. 1a,b**). The firing rate of SNR neurons during a bout of licking was positively correlated with the instantaneous lick rate ($r(38) = 0.94$, $P = 1.53 \times 10^{-19}$; **Fig. 1c**). The lick frequency within bouts (SNR: 7.7 ± 0.06 Hz;

¹Department of Psychology and Neuroscience, Duke University, Durham, North Carolina, USA. ²Department of Cell Biology, Duke University, Durham, North Carolina, USA. ³Center for Cognitive Neuroscience, Duke University, Durham, North Carolina, USA. ⁴Department of Neurobiology, Duke University, Durham, North Carolina, USA. Correspondence should be addressed to H.H.Y. (hy43@duke.edu).

Received 19 January; accepted 10 March; published online 4 April 2016; doi:10.1038/nn.4285

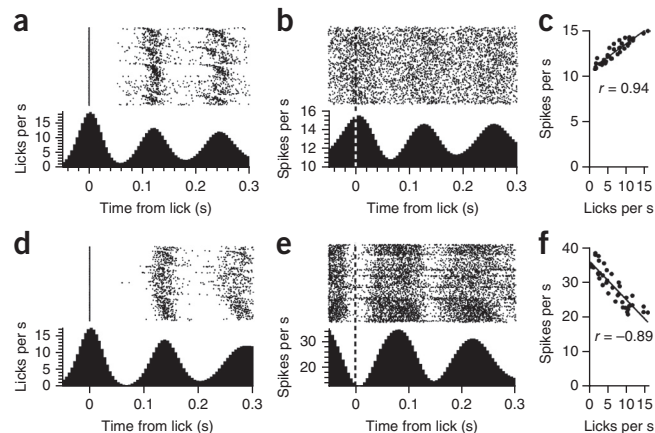
Figure 1 SNR and SC activity is time-locked to the lick cycle. (a) Rate histogram of licks occurring within a bout of licking in a mouse during SNR recording. Licks are aligned to the start of spout contact. Licking proceeded in rhythmic oscillations, shown as peaks and valleys in lick rate. (b) Representative lick-related oscillatory activity of SNR neuron. The oscillations in the neural activity are tightly coupled with the oscillations of the lick cycle. Dashed line indicates the time of spout contact. (c) The firing rate of the neuron in b was positively correlated with instantaneous lick rate, y axis value shown in a ($P = 1.91.53 \times 10^{-19}$). (d) Rate histogram of licks occurring within a bout of licking of a mouse during SC recording. (e) Representative lick-related oscillatory activity of SC neuron. The oscillations in the neural activity were tightly coupled with the oscillations of the lick cycle, but were antiphase to the SNR oscillations. Dashed line indicates the time of spout contact. (f) Firing rate of the neuron in e was negatively correlated with instantaneous lick rate, y axis value shown in d ($P = 8.38 \times 10^{-15}$).

SC: 7.6 ± 0.05 Hz), contact duration (Mann-Whitney $U = 65.00$, $P = 0.53$) and the period of the lick cycle (Mann-Whitney $U = 72.50$, $P = 0.38$) were all extremely consistent across animals (SC, $n = 4$; SNR, $n = 6$; **Supplementary Fig. 1e,f**).

Neurons in the SC also showed oscillatory activity that was tightly coupled with the lick cycle (**Fig. 1d,e**). However, in contrast with the SNR neurons, which were generally in phase with the lick cycle, SC activity was more frequently out of phase with the lick cycle. The activity usually peaked during the retraction phase of the lick cycle, resulting in a strong negative correlation between instantaneous lick rate and spike rate ($r(38) = -0.89$, $P = 8.38 \times 10^{-15}$; **Fig. 1f**).

We quantified the phase relationship between SNR and SC neurons (**Fig. 2a–c**). Many SNR neurons (61%, 53 of 87 neurons from 6 mice) had their peak firing rates at the time of tongue contact (**Fig. 2c**), whereas fewer had their minimum firing rates at the time of spout contact (23%, 20 of 87 neurons from 6 mice). In contrast, few SC neurons (5%, 4 of 74 neurons from 4 mice) showed oscillations that were in phase with licking and peaked at the time of spout contact, whereas a larger proportion (22%, 16 of 74 neurons from 4 mice) were antiphase to the lick cycle and had their minimum response at the time of contact ($\chi^2 = 18.31$, $P = 1.90 \times 10^{-5}$; **Fig. 2d**).

The antiphasic relationship between SNR and SC neural signatures of licking was also evident in the correlation between the instantaneous lick rate and the firing rate (**Fig. 2e**). The activity of many SNR neurons was positively correlated ($P < 0.05$) with lick rate (49%, 43 of 87 neurons from 6 mice). Fewer SNR neurons were negatively correlated with the lick rate (14%, 12 of 87 neurons from 6 mice).



The SC, in contrast, showed the opposite pattern. A greater proportion of neurons were negatively correlated with lick rate (45%, 33 of 74 neurons from 4 mice) than were positively correlated (19%, 14 of 74 neurons from 4 mice; $\chi^2 = 24.08$, $P = 9.20 \times 10^{-7}$).

We also identified neurons in both the SNR and SC that changed their firing rates at the boundaries of a lick bout (**Supplementary Fig. 2**). In each area, we found neurons whose firing rate ramped down before the first lick in a bout ('decreasing neurons') and neurons that ramped up toward the start of a bout ('increasing neurons'). The activity of decreasing neurons was suppressed during a bout of licking and rebounded after licking ceased. The increasing neurons exhibited the opposite pattern: firing rate was elevated during licking and subsided after the bout ended. This is consistent with previous work in rats showing that SNR neurons can exhibit both transient and sustained changes in firing rate before and during licking¹⁹.

Inactivation of lateral SC disrupts licking

Previous studies have implicated the SC in the control of experimentally induced oral stereotypy in rats^{9–11}. However, whether the SC is necessary for initiating voluntary drinking or the patterning of orofacial motor output during voluntary consummatory behavior in mice is less clear. To test this possibility, we injected the GABA-A receptor agonist muscimol into the lateral SC (**Fig. 3a**). In agreement with previous reports in rats¹¹, muscimol dose-dependently suppressed licking in wild-type mice (one-way ANOVA, $F_{(2,6)} = 8.24$, $P = 0.019$; Dunnett's multiple comparison test, vehicle versus $1.0 \mu\text{g} \mu\text{l}^{-1}$ muscimol, $P = 0.04$; **Fig. 3b–d** and **Supplementary Videos 1 and 2**). For mice that were still able to lick following muscimol injections ($n = 3$ mice), the lick duration was increased (one-way ANOVA: $F_{(2,8)} = 20.42$, $P = 0.008$; **Fig. 3e**), although the period was not significantly affected (one-way ANOVA: $F_{(2,8)} = 1.12$, $P = 0.41$; **Fig. 3f**).

On the other hand, when we excitotoxically lesioned the lateral SC of wild-type mice (**Supplementary Fig. 3a,b**), the lesioned mice were

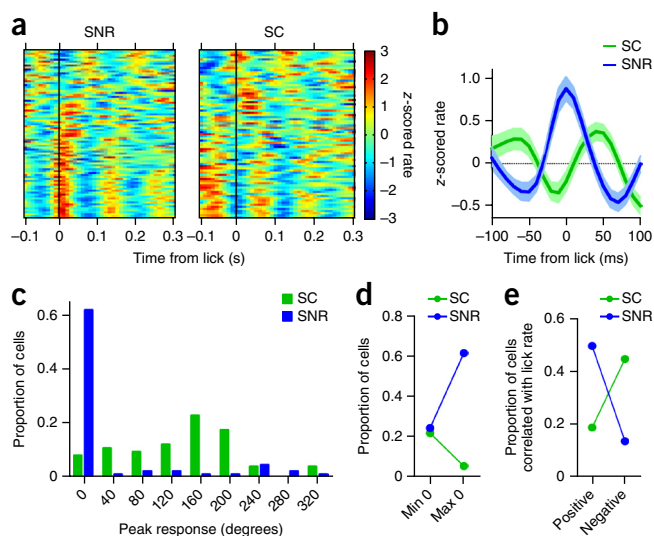
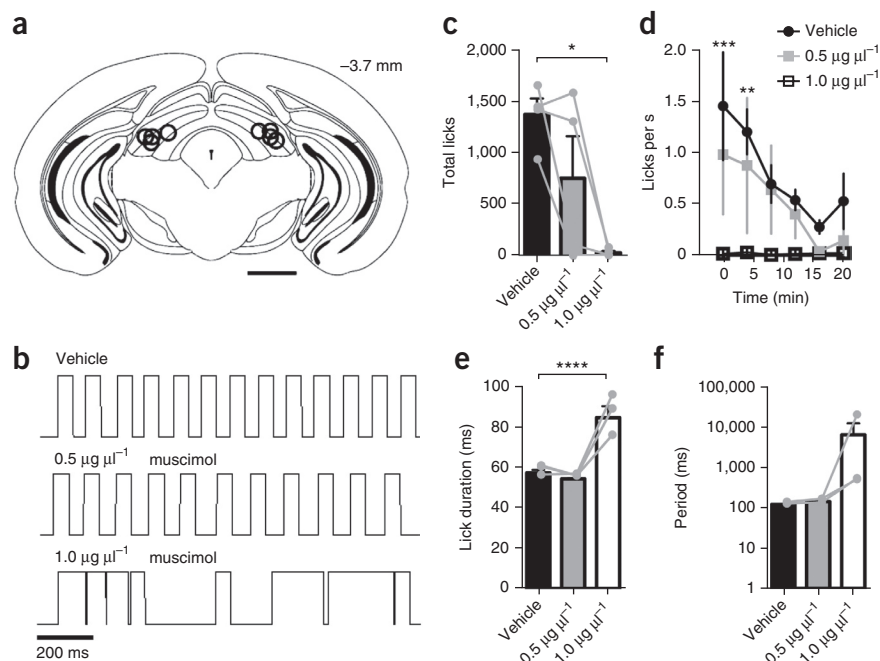


Figure 2 SNR and SC exhibit antiphase oscillations during licking. (a) Population spike density functions showing oscillatory activity of SNR ($n = 87$ neurons from 6 mice) and SC ($n = 74$ neurons from 4 mice) neurons. Each row corresponds to the activity of one neuron. (b) Population average and s.e.m. of neural activity aligned to the start of each lick. (c) Distribution of the point in the lick cycle (in degrees; 0 is the start of contact) of the peak neural response of SNR and SC neurons. (d) Proportion of neurons whose maximum or minimum response rate at the 0 phase of the lick cycle ($\chi^2 = 13.31$, $P = 1.90 \times 10^{-5}$). (e) Proportion of neurons whose firing rate was positively or negatively correlated ($P < 0.05$) with the instantaneous lick rate during a bout of licking ($\chi^2 = 24.08$, $P = 9.20 \times 10^{-7}$).

Figure 3 Muscimol injection into the lateral SC suppresses voluntary licking. (a) Summary of bilateral cannula placements in lateral SC ($n = 4$ mice). Scale bar represents 1 mm. (b) Lick traces from a single mouse following injection of vehicle or muscimol. Upward deflections indicate contact with the lick spout. (c) The number of licks was dose-dependently reduced by muscimol infusion ($*P = 0.019$ vehicle versus $1.0 \mu\text{g } \mu\text{l}^{-1}$ muscimol). (d) Lick rate over time (two-way repeated measures ANOVA, time \times dose: main effect of time ($F_{(7,48)} = 3.75$, $P = 0.007$), main effect of dose ($F_{(2,48)} = 12.95$, $P = 0.00015$), no interaction ($F_{(14,48)} = 1.16$, $P = 0.33$); Bonferroni *post hoc* test, vehicle versus $1.0 \mu\text{g } \mu\text{l}^{-1}$ muscimol at 0 ($***P = 0.0003$) and 4 min ($**P = 0.0021$)). (e,f) For mice that licked at all doses of muscimol ($n = 3$), lick duration was increased ($****P = 0.008$) and the period was not significantly affected ($P = 0.41$). Data are presented as mean and s.e.m. Individual data points are overlaid in gray.



still able to voluntarily drink sucrose solution. The overall rate of licking ($t_{(10)} = 1.45$, $P = 0.18$) and the number of drinking bouts ($t_{(10)} = 0.19$, $P = 0.85$) were unaffected. However, SC lesions still altered the microstructure of licking, significantly increasing the duration of individual licks relative to sham controls ($t_{(10)} = 2.77$, $P = 0.02$) while leaving the period unchanged ($t_{(10)} = 0.79$, $P = 0.45$) (Supplementary Fig. 3c–e). These results suggest that, in the absence of the SC, other descending projections (for example, from the cerebral cortex to brainstem) can assume control and initiate drinking behavior. Alternatively, compensatory changes in the nigrotectal circuit following excitotoxic

lesions can result in functional recovery despite the loss of many neurons. Nevertheless, the nigrotectal projection normally is crucial to self-initiated licking movements.

Nigrotectal activation disrupts consummatory behavior

To visualize nigrotectal projections, we injected a retrogradely transported virus encoding Cre recombinase (Lenti-FuGB2-Cre) into the lateral SC, and a Cre-dependent GFP reporter (AAV-FLEX-GFP) was injected into the SNR²⁰ (Fig. 4a). Because GABAergic and dopaminergic neurons are found in close proximity to one another in the SN, we wanted to confirm that the nigrotectal projection that we studied was GABAergic. Indeed, GFP-expressing nigrotectal neurons colocalized with vesicular GABA transporter (Vgat), but not with tyrosine hydroxylase (TH), a crucial enzyme in dopamine synthesis (Fig. 4b,c).

To determine whether selective perturbation of GABAergic nigrotectal neurons can alter behavioral output, we expressed Cre-dependent channelrhodopsin-2 (ChR2) bilaterally in the SNR of Vgat-Cre mice (mice expressing Cre recombinase under the control of the *Vgat* (also known as *Slc32a1*) promoter; $n = 7$) and targeted the axon terminals in the lateral SC with optic fibers (Vgat::ChR2^{SNR→SC}; Supplementary Fig. 4). ChR2 was restricted to non-dopaminergic neurons in the SNR (Fig. 4d–f). ChR2-expressing terminals were found in the SC and were particularly dense in the lateral region. Fluorescence intensity was similar between the SN and

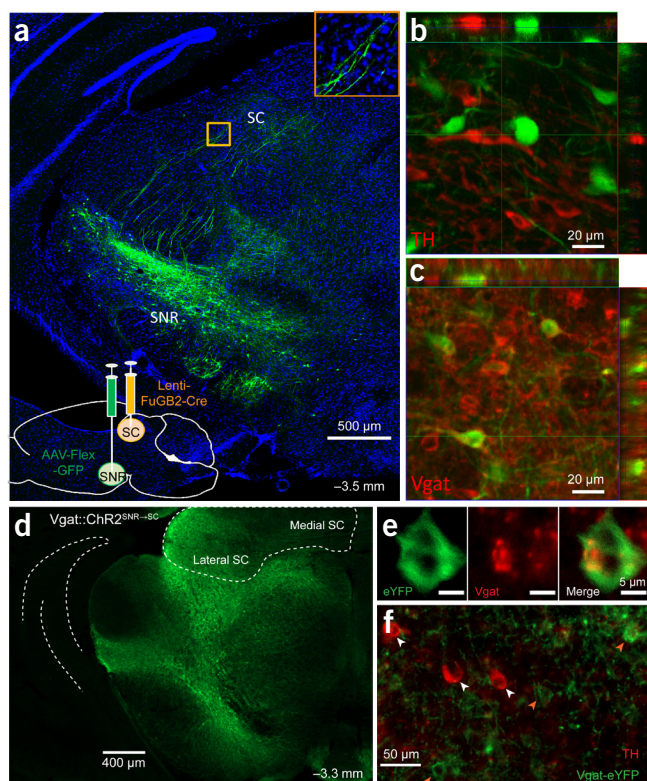
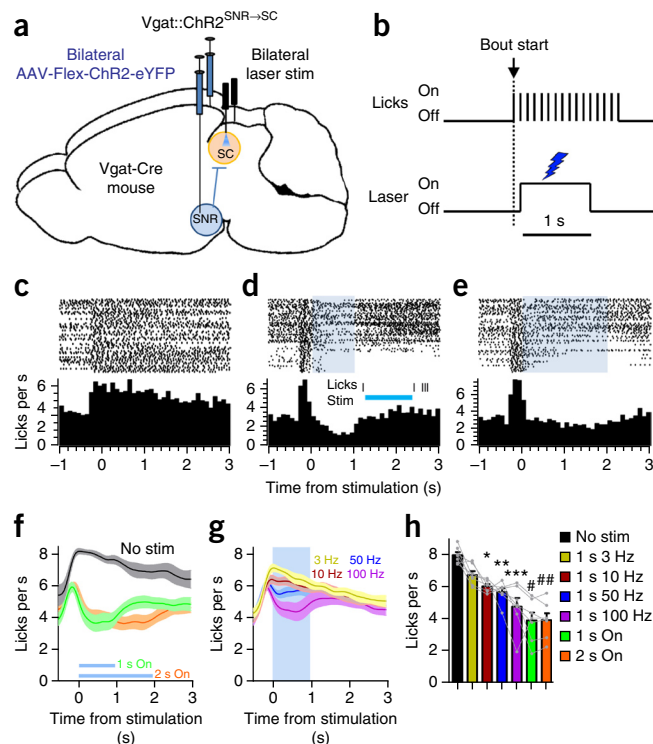


Figure 4 SNR GABA neurons project to lateral SC. (a) Lenti-FuGB2-Cre was injected into lateral SC yielding retrogradely transported Cre. AAV-Flex-GFP was injected in SNR, resulting in selective expression of GFP in nigrotectal neurons. Bottom inset shows nigrotectal axons in the lateral SC. (b) No overlap was observed between TH-expressing and GFP-expressing neurons. (c) GFP colocalized with Vgat-expressing neurons. The experiment was conducted in a single mouse. (d–f) Nigrotectal projections were targeted with ChR2. AAV-Flex-ChR2-eYFP was injected into the SNR of Vgat-Cre mice. Optic fibers targeted the nigrotectal axons in the lateral SC. (d) Example of Vgat-ChR2-eYFP expression. (e) eYFP overlapped with Vgat. (f) eYFP did not overlap with TH. The experiment was successfully repeated on seven mice.

Figure 5 $Vgat::ChR2^{SNR \rightarrow SC}$ activation disrupts consummatory behavior. (a) Schematic representation of optogenetic stimulation strategy. Cre-dependent ChR2 was bilaterally injected into the SNR of $Vgat$ -Cre mice ($n = 7$). Optic fibers targeted nigroreticular axon terminals in the lateral SC. (b) Depiction of lick-triggered optogenetic stimulation. A computer program triggered the laser after the start of a licking bout. (c–e) Peri-stimulation lick plots from one mouse. When no stimulation was present (c), the lick rate remained elevated following the initiation of a lick bout. When 1 s (d) or 2 s (e) of constant illumination (~ 10 mW) was delivered during a bout, licking was temporarily interrupted and rebounded following the termination of stimulation. The inset in d is a single-trial example of when licking was completely abolished during stimulation. (f,g) Group ($n = 7$ mice) average (\pm s.e.m.) peri-stimulus lick rate with constant (f) or pulsed (g) illumination. (h) Lick rate during stimulation decreased as a function of stimulation frequency. * $P = 0.04$, ** $P = 0.018$, *** $P = 0.003$, # $P = 8.88 \times 10^{-4}$, ## $P = 9.00 \times 10^{-4}$ compared with no-stimulation condition. Error bars represent mean + s.e.m.



lateral SC, but was lower in the medial SC compared with both the SNR and lateral SC (Supplementary Fig. 4b).

For optogenetic experiments, laser stimulation was triggered by contact with the spout (Fig. 5a,b). Constant illumination of the nigroreticular projections markedly reduced the number of licks for the duration of the stimulation (Fig. 5c–f). $Vgat::ChR2^{SNR \rightarrow SC}$ stimulation reduced the lick rate in a frequency-dependent manner (one-way repeated-measures ANOVA, $F_{(6,36)} = 19.55$, $P = 5.42 \times 10^{-10}$; Dunnett's multiple comparison test, no stimulation versus 10 Hz ($P = 0.04$), 50 Hz ($P = 0.018$), 100 Hz ($P = 0.003$), 1 s on ($P = 8.88 \times 10^{-4}$) and 2 s on ($P = 9.00 \times 10^{-4}$); Fig. 5g,h). Thus, high-frequency stimulation, as well as constant illumination, were most effective at disrupting licking.

$Vgat::ChR2^{SNR \rightarrow SC}$ stimulation did not affect the overall lick rate (Supplementary Fig. 5a), but instead altered the pattern of licking. Stimulation increased the number of licking bouts (Supplementary Fig. 5b) and reduced the number of licks per bout (Supplementary Fig. 5c). The mean lick duration was unaffected (Supplementary Fig. 5d), but the variability of lick durations was increased by stimulation (Supplementary Fig. 5e). This is consistent with stimulation transiently interrupting the motor output associated with consummatory behavior. Moreover, the efficacy of stimulation was affected by motivational state. When mice were less motivated to drink near the end of the session, stimulation was especially effective at inhibiting licking (Supplementary Fig. 5f).

To test whether nonspecific effects of laser illumination or viral infection contributed to the reduced licking rate during $Vgat::ChR2^{SNR \rightarrow SC}$ stimulation, we injected $Vgat$ -Cre mice ($n = 6$) with the AAV-FLEX-YFP control vector ($Vgat::YFP^{SNR \rightarrow SC}$). Under similar experimental conditions, laser stimulation in the absence of ChR2 had no effect on the lick rate (Supplementary Fig. 6).

Stimulation effects on other orofacial behaviors

Since the SC has been implicated in head movement and orienting behavior^{11,21}, we asked whether the $Vgat::ChR2^{SNR \rightarrow SC}$ stimulation used to disrupt orofacial behavior caused aberrant head movements, which could explain the suppression of licking. Licking was often not completely abolished by stimulation, but was rather slowed with an irregular pattern (Figs. 5d,e). Thus, the mice were not completely breaking contact with the spout, as would be expected if stimulation produced rearing or head turning. To quantify whether nigroreticular stimulation induced head movement, we stimulated $Vgat::ChR2^{SNR \rightarrow SC}$ and $Vgat::YFP^{SNR \rightarrow SC}$ mice while tracking the mice's heads with three-dimensional motion capture at 100 frames per second (Online Methods). There was no effect of stimulation

on head movement (Supplementary Fig. 7). In addition, we used a head-fixed preparation, in which precise orofacial movements, such as vibrissae whisking and eye blinks in response to photo-stimulation, could be quantified. In head-fixed mice, $Vgat::ChR2^{SNR \rightarrow SC}$ stimulation reduced licking in a frequency-dependent manner (Supplementary Fig. 8a,b and Supplementary Video 3) without affecting whisking or blinking (Supplementary Fig. 8c,d and Supplementary Video 4). These results indicate that stimulation of the lateral nigroreticular pathway studied here has a selective effect on drinking behavior.

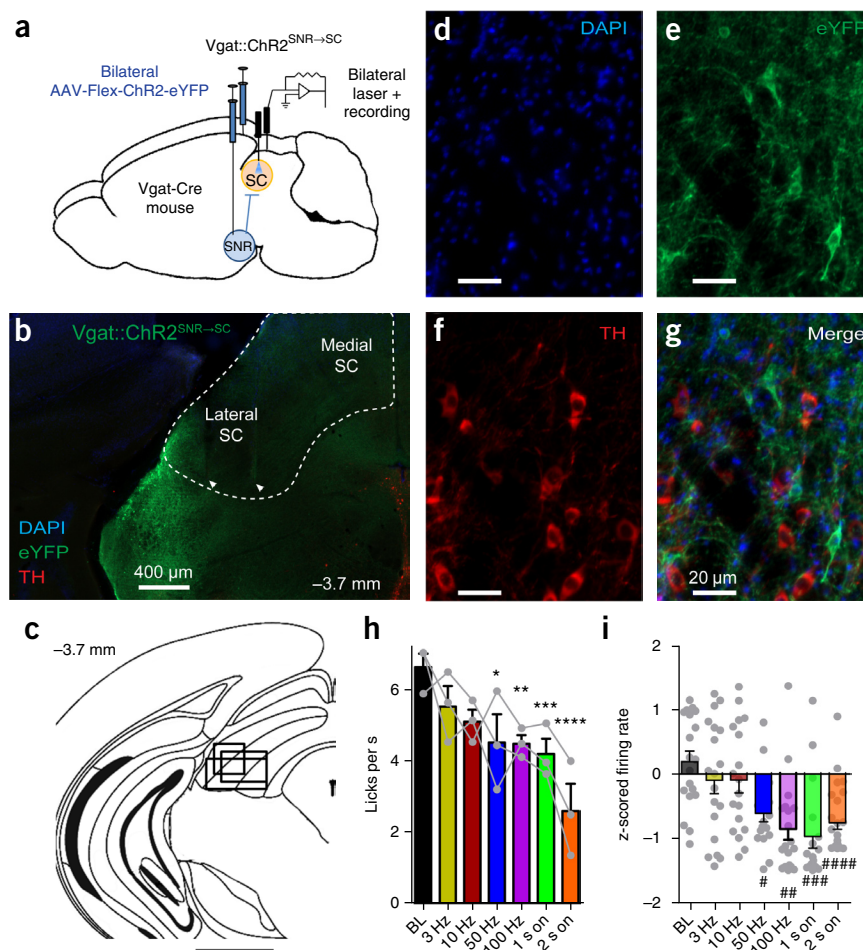
Nigro-mRF activation does not alter consummatory behavior

SNR neurons are known to project to the mesencephalic reticular formation (mRF), which is located ventral to the site of SC stimulation. Because some nigroreticular neurons can send axon collaterals to the reticular formation⁸, and because our optic fibers are located close to the mRF, it is possible that the nigro-mRF projections, rather than the nigroreticular projections, are responsible for the observed effects. We therefore tested whether optogenetic activation of $Vgat^{SNR \rightarrow mRF}$ projections is sufficient to account for the observed effects of $Vgat^{SNR \rightarrow SC}$ activation (Supplementary Fig. 9). Unlike $Vgat::ChR2^{SNR \rightarrow SC}$ stimulation, $Vgat::ChR2^{SNR \rightarrow mRF}$ stimulation did not affect lick rate when mice voluntarily drank sucrose solution (Supplementary Fig. 10). This further supports a specific role of nigroreticular projections in regulating consummatory drinking.

Nigroreticular activation inhibits SC neurons to disrupt licking

To understand the effect that $Vgat::ChR2^{SNR \rightarrow SC}$ stimulation has on the SC, we performed extracellular recordings from neurons in the SC during optogenetic activation of nigroreticular neurons while mice ($n = 3$) consumed sucrose solution (Fig. 6a–g). As in the previous experiment, $Vgat::ChR2^{SNR \rightarrow SC}$ activation suppressed licking in a frequency-dependent manner (one-way ANOVA, $F_{(6,12)} = 6.29$, $P = 0.0035$; Dunnett's multiple comparison test, baseline versus

Figure 6 *Vgat::ChR2^{SNR→SC}* stimulation inhibits SC neurons and suppresses consummatory behavior. **(a)** Schematic representation of optrode recording strategy. Cre-dependent ChR2 was bilaterally injected into the SNR of *Vgat-Cre* mice ($n = 3$). An optic fiber was placed in the SC of one hemisphere and an optrode in the other. **(b)** Representative placement of optrode in the lateral SC. Electrode locations are indicated by arrowheads. The SC is outlined in white dashed line. **(c)** The spread of electrode placements is indicated by a single rectangle corresponding to each mouse. Scale bar represents 1 mm. **(d–g)** eYFP-expressing neurons did not overlap with TH-expressing neurons. In **b** and **d–g**, the experiment was successfully repeated on three mice. **(h)** *Vgat::ChR2^{SNR→SC}* stimulation reduced lick rate. **(i)** SC population activity was suppressed by *Vgat::ChR2^{SNR→SC}* activation ($n = 135$ units recorded from 3 mice). * $P = 0.007$, ** $P = 0.006$, *** $P = 0.002$, **** $P = 7.8 \times 10^{-5}$, # $P = 6.0 \times 10^{-5}$, ## $P = 5.65 \times 10^{-3}$, ### $P = 1.02 \times 10^{-4}$, #### $P = 1.86 \times 10^{-4}$ compared to BL. Error bars represent s.e.m.



50 Hz ($P = 0.007$), 100 Hz ($P = 0.006$), 1 s on ($P = 0.002$) and 2 s on ($P = 7.8 \times 10^{-5}$; **Fig. 6h**). This was accompanied by a suppression of SC neuron activity ($F_{(6,134)} = 7.37$, $P = 7.12 \times 10^{-7}$; Dunnett's multiple comparison test, baseline versus 50 Hz ($P = 6.0 \times 10^{-5}$), 100 Hz ($P = 5.65 \times 10^{-3}$), 1 s on ($P = 1.02 \times 10^{-4}$) and 2 s on ($P = 1.86 \times 10^{-4}$; **Fig. 6i**). In accord with the hypothesis that GABAergic SNR neurons inhibit downstream targets, the activity of SC neurons (65%, 11 of 17 neurons from 3 mice) was transiently suppressed during constant illumination (paired t test of spike rate during stimulation versus rate immediately before stimulation, $P < 0.05$; **Fig. 7a–c**). The spike rate of these neurons was reduced during the stimulation epoch and rebounded immediately after stimulation ceased (planned comparison paired t tests before stimulation versus during, $t_{(10)} = 50.62$, $P = 2.19 \times 10^{-13}$; during stimulation versus after, $t_{(10)} = 10.78$, $P = 7.93 \times 10^{-7}$; **Fig. 7b**). When the activity of SC neurons was optogenetically suppressed (t test using the activity from all trials in the session, $t_{(34)} = 3.85$, $P = 0.0005$; **Fig. 7d–f**), the lick rate was also suppressed (t test with Welch's correction for unequal variance, $t_{(31)} = 6.27$, $P = 5.31 \times 10^{-7}$; **Fig. 7g–i**). *Vgat::ChR2^{SNR→SC}* stimulation also suppressed SC activity when mice were not licking (**Supplementary Fig. 11**).

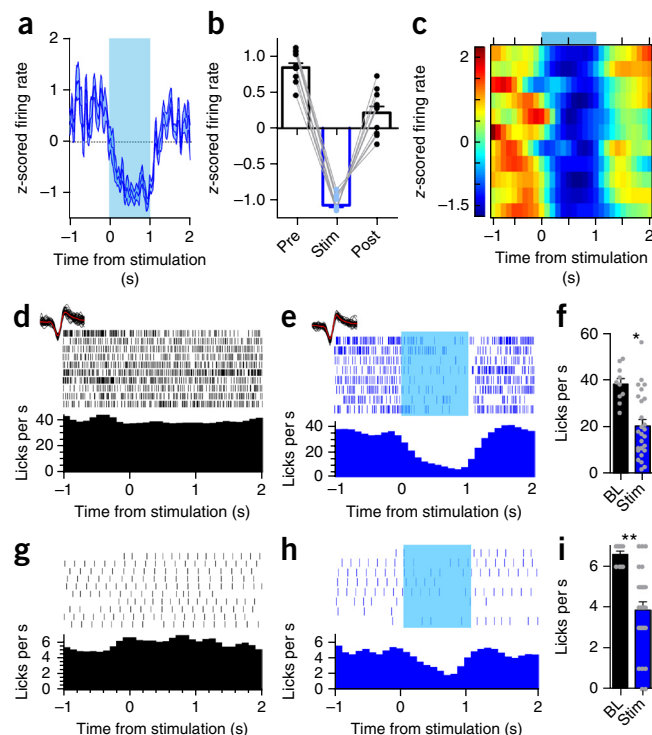
Since many SC neurons showed oscillatory activity that was antiphase to the lick cycle (**Fig. 2b**), we measured the effect of *Vgat::ChR2^{SNR→SC}* stimulation on such activity. Similar to the previous recordings, SC neurons recorded in optrode experiments showed oscillatory activity that was roughly 180 degrees out of phase with the lick cycle (36%, 28 of 78 neurons from 3 mice). On trials in which licking was not eliminated by stimulation, the lick-related oscillatory activity of SC neurons was disrupted by photostimulation (**Supplementary Figs. 12 and 13**). The amplitude of neural oscillations was suppressed by *Vgat::ChR2^{SNR→SC}* stimulation (**Supplementary Fig. 13h**). In addition, the phase relationship was also altered (**Supplementary Fig. 13i–k**).

DISCUSSION

We found that neurons in both the substantia nigra and the SC exhibit oscillatory activity reflecting the pattern of consummatory drinking behavior. Selective optogenetic stimulation of the direct GABAergic projection from SNR to SC disrupted licking-related oscillatory activity as well as consummatory behavior. These data suggest a role for nigroreticular projections in selectively regulating orofacial behavior and suggest that the recorded SC neurons are downstream of SNR lick-related neurons. Most lateral SNR output neurons fired in phase with the lick cycle, their firing rates peaking at the time of spout contact. Most neurons in the lateral SC showed antiphase activity, peaking when the tongue was retracted. This pattern can be explained by the GABAergic projections from the SNR to the SC (**Fig. 4**). ChR2-mediated activation of this GABAergic nigroreticular projection suppressed lick-related activity of SC neurons and stopped licking (**Figs. 6 and 7**).

Together, these results suggest that the nigroreticular pathway has a critical role in voluntary drinking behavior. Our findings reveal, to the best of our knowledge for the first time, a precise quantitative relationship between a set of SNR and SC neurons. They are also consistent with previous work showing inhibitory effects of nigral neurons on collicular neurons in eye movements^{22,23}. However, the oculomotor-related neurons represent only a minority of nigral neurons²⁴. In rodents, the nigroreticular projections serve many other important functions. Just as eye movements serve to acquire the appropriate visual sensory input, other systems can control the position of the

Figure 7 When $Vgat::ChR2^{SNR \rightarrow SC}$ stimulation inhibits SC neurons, consummatory behavior is suppressed. (a–c) 65% (11 of 17 neurons from 3 mice) of neurons were inhibited during 1-s constant illumination. (a) Average response of all inhibited neurons. (b) Inhibition was transient and spike rates rebounded immediately after stimulation. (c) Spike density function showing activity of inhibited neurons during stimulation. (d,e) Single-unit activity recorded during licking. (d) The neuron was tonically active during licking on baseline trials in which the laser was off. (e) Constant illumination during licking suppressed firing. Waveforms recorded during baseline trials and when the laser was on are shown above the rasters (red lines are median waveforms). Waveform shape was unchanged by laser. (f) This neuron was inhibited by $Vgat::ChR2^{SNR \rightarrow SC}$ stimulation (t test, 10 baseline trials and 26 stimulation trials: $t_{(34)} = 3.85$, $*P = 0.0005$). (g) Licking behavior during the trials shown in a. (h) When the laser was on, the lick rate was suppressed. (i) Lick rate was significantly reduced by $Vgat::ChR2^{SNR \rightarrow SC}$ stimulation (t test with Welch's correction for unequal variance, 10 baseline trials and 26 stimulation trials: $t_{(31)} = 6.27$, $**P = 5.31 \times 10^{-7}$). Data are presented as mean \pm s.e.m.



relevant sensors (for example, tactile and taste) to acquire their respective inputs. The tectum therefore contains multiple target acquisition systems for distinct sensory modalities, altering the positions of sensors all over the body. What is unique about drinking is that a relatively fixed action pattern is generated in the behavioral output. A bout of licks with a stereotyped frequency and usually persisting for a few seconds is the basic unit of perceptual sampling.

In rodents, the SC is somatotopically organized such that the most lateral region receives input from the mouth and face²⁵. The deep layers of the lateral SC (Fig. 4) may be dedicated to orofacial movements. Although the nigrotectal pathway has been implicated in orienting behavior in rodents and primates⁹, we did not observe any stimulation to induce head turning (Supplementary Fig. 7), whisking (Supplementary Fig. 8c) or blinking (Supplementary Fig. 8d). It is possible that other tectal regions (for example, the medial SC) are important for these functions. The SNR also sends axon collaterals to the mRF and thalamus. Stimulation of the SNR projections to the mRF did not affect licking (Supplementary Fig. 10), but we cannot rule out the possibility that optogenetic activation of nigrothalamic projections contributes to the observed effects.

When the SC was temporarily inactivated with muscimol or with activation of the GABAergic nigrotectal pathway, licking was abolished, demonstrating the necessity of this region for voluntary licking. Yet mice were still able to lick following SC lesions, albeit with disrupted patterning. This recovery of function can be attributed to changes in other pathways that are also involved in voluntary licking. For example, the well-known descending projections from the orofacial region in the motor cortex may be used as an alternative pathway by which descending commands can be issued in voluntary drinking^{12,26,27}. However, little is known about the interactions between the descending cortical and nigrotectal pathways, and the distinction between their respective contributions remains unclear.

It is possible that optogenetic stimulation of the nigrotectal pathway reduces motivation to consume the sucrose reward. The time course of the behavioral response, however, makes this possibility unlikely. Motivational effects on neural activity tend to act slowly, gradually changing appetitive behavior²⁸. The reduction in lick rate occurred abruptly and transiently within the stimulation epoch. Moreover, repeated stimulations did not alter the overall lick rate for the entire session (Supplementary Fig. 5a), but rather interrupted an ongoing bout of licking (Supplementary Fig. 5b,c). For these reasons, the

effects of photo-stimulation are likely restricted to the initiation of the orofacial motor pattern generation. Motivationally relevant signals can probably influence licking behavior at a higher level, such as the corticostriatal pathway. Such modulation will not directly affect the production of individual licks, but rather mainly the initiation and termination of the lick pattern generator.

In rodents, neurons in the lateral part of the superior colliculus located near the site of termination of the nigrotectal axons send projections to the medullary reticular formation^{26,29,30}, which is the site of oral premotor neurons^{3,31,32}. The premotor neurons in the reticular formation make connections with hypoglossal motor neurons, which target the tongue muscles. The projections from the lateral SNR to the lateral SC are thus anatomically positioned to contribute to the generation of oral behaviors. Neurons in the reticular formation and the hypoglossal nucleus exhibit oscillatory activity similar to that which we observed—tightly coupled with the lick cycle^{31,33,34}. However, the activity of reticular neurons that are rhythmically active during licking is distributed throughout the lick cycle³¹. Thus, it remains to be tested how the oscillatory patterns observed in the SNR and SC can be related to specific activity patterns of oral motor and premotor neurons.

One important question is whether the nigrotectal pathway is important for orofacial behaviors other than licking. If nigrotectal stimulation simply elicited competing behaviors, for example, then there would be a trivial explanation for suppressed drinking. We found that optogenetic stimulation of the nigrotectal pathway, which suppressed voluntary licking, had no effect on blinking or whisking (Supplementary Fig. 8), behaviors that are thought to be controlled by the SC, but do not usually rely on the same effectors as licking.

Compared with other orofacial behaviors, licking is more easily measurable and quantifiable. But even licking involves the coordination of many different effectors, such as muscles that open and close the mouth. It probably shares many premotor and motor neurons with

other orofacial behaviors. Although we were not able to measure other behaviors such as chewing, the same nigrotectal pathway could be involved as well, to the extent that some of the effectors are shared.

It is also instructive to compare licking with more extensively studied behaviors such as eye movements, which rely on more medial parts of the SNR and SC. To generate a saccade, coordinated activity of many SC neurons is needed to acquire the signal from a specific location in the visual field, corresponding to a particular visual target. In the case of licking, it is possible that the perceptual signal acquired by varying SC output is not contact with the target, but rather proprioceptive information related to tongue position. Thus, the controlled variable for this circuit is likely tongue position (protrusion and retraction), although taste cannot be ruled out. On the other hand, the controlled variable for the medial SC circuit is the position of visual input on a retinotopically organized map field. In addition, other related nigrotectal circuits may coordinate the acquisition of somatosensory information from the body surface and vibrissae. In each case, directed movements of different body parts achieve specific orientation of some sensor with respect to some distal or proximal target, thereby controlling the input quantity continuously. The basic computation is similar, despite differences in what the perceptual inputs represent.

It is therefore possible that lick-related nigral activity can specify tongue position in relation to some target for downstream systems, and the target tectal neurons compare these descending reference signals with their own sensory feedback, using the discrepancy to influence brainstem circuits responsible for lick pattern generation. This allows descending signals from the cerebrum to modify and command the activity of central pattern generators in the brainstem. This is supported by recent work demonstrating that the firing rates of SNR GABA neurons reflect instantaneous position coordinates of the head during behavior³⁵. However, current technology does not allow precise continuous measurements of tongue position. This hypothesis remains to be tested using more advanced behavior tracking techniques.

METHODS

Methods and any associated references are available in the [online version of the paper](#).

Note: Any Supplementary Information and Source Data files are available in the online version of the paper.

ACKNOWLEDGMENTS

We would like to thank F. Wang, L. Glickfeld, and G. Stuber for help with the head-fixed setup. This research is supported by US National Institutes of Health grant MH103374 (S.H.S.), AA021074 (H.H.Y.), and National Science Foundation graduate fellowships (M.A.R. and J.W.B.).

AUTHOR CONTRIBUTIONS

M.A.R. and H.H.Y. conceived the study, analyzed the data and wrote the manuscript. M.A.R., H.E.L., D.L., R.A.B., E.G., J.W.B., N.K., and M.T.C. performed the behavioral experiments. M.A.R. and H.E.L. performed the electrophysiological recordings. I.H.K. and S.H.S. performed the viral tracing and imaging.

COMPETING FINANCIAL INTERESTS

The authors declare no competing financial interests.

Reprints and permissions information is available online at <http://www.nature.com/reprints/index.html>.

1. Fowler, S.C. & Mortell, C. Low doses of haloperidol interfere with rat tongue extensions during licking: a quantitative analysis. *Behav. Neurosci.* **106**, 386–395 (1992).
2. Nakamura, S., Muramatsu, S. & Yoshida, M. Role of the basal ganglia in manifestation of rhythmic jaw movement in rats. *Brain Res.* **535**, 335–338 (1990).
3. Travers, J.B., Dinardo, L.A. & Karimnamazi, H. Motor and premotor mechanisms of licking. *Neurosci. Biobehav. Rev.* **21**, 631–647 (1997).

4. Alexander, G.E. & Crutcher, M.D. Functional architecture of basal ganglia circuits: neural substrates of parallel processing. *Trends Neurosci.* **13**, 266–271 (1990).
5. Yin, H.H., Ostlund, S.B. & Balleine, B.W. Reward-guided learning beyond dopamine in the nucleus accumbens: the integrative functions of cortico-basal ganglia networks. *Eur. J. Neurosci.* **28**, 1437–1448 (2008).
6. Takakusaki, K., Saitoh, K., Harada, H. & Kashiwayanagi, M. Role of basal ganglia-brainstem pathways in the control of motor behaviors. *Neurosci. Res.* **50**, 137–151 (2004).
7. Deniau, J.M. & Chevalier, G. The lamellar organization of the rat substantia nigra pars reticulata: distribution of projection neurons. *Neuroscience* **46**, 361–377 (1992).
8. Beckstead, R.M. Long collateral branches of substantia nigra pars reticulata axons to thalamus, superior colliculus and reticular formation in monkey and cat. Multiple retrograde neuronal labeling with fluorescent dyes. *Neuroscience* **10**, 767–779 (1983).
9. Taha, E.B., Dean, P. & Redgrave, P. Oral behaviour induced by intranigral muscimol is unaffected by haloperidol but abolished by large lesions of superior colliculus. *Psychopharmacology (Berl.)* **77**, 272–278 (1982).
10. Redgrave, P., Dean, P., Donohoe, T.P. & Pope, S.G. Superior colliculus lesions selectively attenuate apomorphine-induced oral stereotypy: a possible role for the nigrotectal pathway. *Brain Res.* **196**, 541–546 (1980).
11. Wang, S. & Redgrave, P. Microinjections of muscimol into lateral superior colliculus disrupt orienting and oral movements in the formalin model of pain. *Neuroscience* **81**, 967–988 (1997).
12. Li, N., Chen, T.-W., Guo, Z.V., Gerfen, C.R. & Svoboda, K. A motor cortex circuit for motor planning and movement. *Nature* **519**, 51–56 (2015).
13. Bjursten, L.M., Norrsell, K. & Norrsell, U. Behavioural repertoire of cats without cerebral cortex from infancy. *Exp. Brain Res.* **25**, 115–130 (1976).
14. Bignall, K.E. & Schramm, L. Behavior of chronically decerebrate kittens. *Exp. Neurol.* **42**, 519–531 (1974).
15. Grill, H.J. Production and regulation of ingestive consummatory behavior in the chronic decerebrate rat. *Brain Res. Bull.* **5**, 79–87 (1980).
16. Rossi, M.A. & Yin, H.H. Elevated dopamine alters consummatory pattern generation and increases behavioral variability during learning. *Front. Integr. Neurosci.* **9**, 37 (2015).
17. Spector, A.C., Klumpp, P.A. & Kaplan, J.M. Analytical issues in the evaluation of food deprivation and sucrose concentration effects on the microstructure of licking behavior in the rat. *Behav. Neurosci.* **112**, 678–694 (1998).
18. Weijnen, J.A. Licking behavior in the rat: measurement and situational control of licking frequency. *Neurosci. Biobehav. Rev.* **22**, 751–760 (1998).
19. Gulley, J.M., Kosobud, A.E. & Rebec, G.V. Behavior-related modulation of substantia nigra pars reticulata neurons in rats performing a conditioned reinforcement task. *Neuroscience* **111**, 337–349 (2002).
20. Kim, I.H. *et al.* Spine pruning drives antipsychotic-sensitive locomotion via circuit control of striatal dopamine. *Nat. Neurosci.* **18**, 883–891 (2015).
21. Redgrave, P., Marrow, L. & Dean, P. Topographical organization of the nigrotectal projection in rat: evidence for segregated channels. *Neuroscience* **50**, 571–595 (1992).
22. Chevalier, G., Deniau, J.M., Thierry, A.M. & Feger, J. The nigro-tectal pathway. An electrophysiological reinvestigation in the rat. *Brain Res.* **213**, 253–263 (1981).
23. Hikosaka, O. & Wurtz, R.H. Visual and oculomotor functions of monkey substantia nigra pars reticulata. IV. Relation of substantia nigra to superior colliculus. *J. Neurophysiol.* **49**, 1285–1301 (1983).
24. DeLong, M.R., Crutcher, M.D. & Georgopoulos, A.P. Relations between movement and single cell discharge in the substantia nigra of the behaving monkey. *J. Neurosci.* **3**, 1599–1606 (1983).
25. Dräger, U.C. & Hubel, D.H. Topography of visual and somatosensory projections to mouse superior colliculus. *J. Neurophysiol.* **39**, 91–101 (1976).
26. Tsumori, T., Ono, K., Kishi, T. & Yasui, Y. Demonstration of the corticotectobulbar pathway from the orofacial motor cortex to the parvocellular reticular formation in the rat. *Brain Res.* **755**, 151–155 (1997).
27. Komiya, T. *et al.* Learning-related fine-scale specificity imaged in motor cortex circuits of behaving mice. *Nature* **464**, 1182–1186 (2010).
28. Rossi, M.A., Fan, D., Barter, J.W. & Yin, H.H. Bidirectional modulation of substantia nigra activity by motivational state. *PLoS One* **8**, e71598 (2013).
29. Yasui, Y. *et al.* Descending projections from the superior colliculus to the reticular formation around the motor trigeminal nucleus and the parvocellular reticular formation of the medulla oblongata in the rat. *Brain Res.* **656**, 420–426 (1994).
30. Tsumori, T. & Yasui, Y. Organization of the nigro-tecto-bulbar pathway to the parvocellular reticular formation: a light- and electron-microscopic study in the rat. *Exp. Brain Res.* **116**, 341–350 (1997).
31. Travers, J.B., DiNardo, L.A. & Karimnamazi, H. Medullary reticular formation activity during ingestion and rejection in the awake rat. *Exp. Brain Res.* **130**, 78–92 (2000).
32. Stanek, E. IV, Cheng, S., Takatoh, J., Han, B.X. & Wang, F. Monosynaptic premotor circuit tracing reveals neural substrates for oro-motor coordination. *Elife* **3**, e02511 (2014).
33. Wiesenfeld, Z., Halpern, B.P. & Tapper, D.N. Licking behavior: evidence of hypoglossal oscillator. *Science* **196**, 1122–1124 (1977).
34. Nakamura, Y., Enomoto, S. & Kato, M. The role of medial bulbar reticular neurons in the orbital cortically induced masticatory rhythm in cats. *Brain Res.* **202**, 207–212 (1980).
35. Barter, J.W. *et al.* Basal ganglia outputs map instantaneous position coordinates during behavior. *J. Neurosci.* **35**, 2703–2716 (2015).

ONLINE METHODS

Subjects. For optogenetic stimulation experiments, Vgat-IRES-Cre mice (*Slc32a1^{tm2(cre)Low}*)³⁶ aged 3–15 months at the start of experiments were used. For SN recordings, male C57BL/6 mice ($n = 6$; 4–6 months) were used. For SC recordings, C57BL/6 ($n = 4$; 4–6 months, two female) were used. For the SC lesion experiment, C57BL/6 mice ($n = 12$; 2 months, three female) were used. All mice were naive before surgery. Mice were maintained on a 12:12 light cycle and were given *ad libitum* food in their home cages. Except where indicated, mice were maintained on a 22.5-h water deprivation schedule. During testing, water was restricted. Mice were allowed to freely consume sucrose solution during licking tests and were given access to water for 1 h following all recording sessions. Food was available at all times in the home cages. All experiments were conducted during the light phase of the animal's light cycle. All experiments were approved by the Duke University Institutional Animal Care and Use Committee guidelines.

Surgery. Virus injection. For optogenetics experiments, mice were anesthetized with isoflurane (induction at 3%, maintained at 1%) and headfixed in a stereotaxic frame (Kopf). Craniotomies were made bilaterally above the lateral SN. Mice were randomly assigned to ChR2 or YFP groups.

For Vgat^{SNR→SC} stimulation, 0.5 μ l of AAV-EF1 α -DIO-ChR2(H134R)-eYFP (ChR2; $n = 7$, 4 male) or the control vector AAV-EF1 α -DIO-eYFP ($n = 6$; 4 male) was injected with a microsyringe over 10 min into the SNR targeting the coordinates (in mm relative to Bregma): AP -3.2 , ML ± 1.6 , DV -4.3 from brain surface. Custom-made optic fibers were then implanted targeting the lateral superior colliculus (AP -3.5 , ML ± 1.3 , DV -2.0). Mice were group housed 2–5 per cage.

For Vgat^{SNR→mRF} stimulation, 0.5 μ l of AAV-EF1 α -DIO-ChR2(H134R)-eYFP (ChR2; $n = 6$, all male) or the control vector AAV-EF1 α -DIO-eYFP ($n = 5$, all male) was injected with a microsyringe over 10 min into the SNR. Optic fibers were implanted bilaterally targeting the mesencephalic reticular formation (mRF) at -4.0 AP, ± 1.0 ML, and -3.0 DV (in mm relative to Bregma). Fibers were secured in place with dental acrylic and skull screws. Mice were allowed to recover for at least 2 weeks before testing began. Mice were group housed 2–5 per cage.

Electrode implantation. Mice were anesthetized and headfixed. A craniotomy was made above the site targeting the SNR (4 left, 2 right) and dura was removed. Electrode arrays (16-channel, 4×4 tungsten microwires, 35- μ m diameter, 150- μ m electrode spacing, 200- μ m row spacing, 6-mm length; Innovative Neurophysiology) were lowered into place in the SN. A silver ground wire was secured to the skull screws and the array was secured in place with dental acrylic. Mice were implanted in the SN or the SC targeting the above coordinates. Procedures were the same for SC implants except the electrodes were custom made 4-mm-long tungsten microwire arrays. Mice were singly housed after surgery.

Optrode implantation. Vgat-Cre mice were injected with ChR2 as described above. In one hemisphere, an optic fiber was implanted targeting the lateral SC. An optrode was implanted in the opposite hemisphere ($n = 3$). The optrode was a custom made 4-mm-long, 4×4 tungsten microwire array with an optic fiber attached to the lateral side and angled so the cone of the emitted light encompassed the electrode tips constructed as previously described³⁷. All cranial implants were secured in place with dental acrylic and skull screws. Mice were allowed to recover for at least 2 weeks before testing began. Mice were singly housed after surgery.

Excitotoxic lesions of lateral SC. C57BL/6 mice (aged 6–9 weeks) were injected with either 0.25 μ l per hemisphere of 2.5 mg ml⁻¹ NMDA (lesion group: $n = 6$, 1 female) dissolved in PBS or with PBS only (sham group: $n = 5$, 2 female) targeting the lateral SC. Mice were randomly assigned to either lesion or sham group. Injections were made at a rate of 0.1 μ l min⁻¹ and the syringe was left in place for 5 min after the injection. To reduce the severity of seizures resulting from excessive stimulation of the deep layers of the SC^{38,39}, all mice were treated with 2.0 mg per kg of body weight of the anticonvulsant diazepam (i.p.) immediately following surgery. Mice were allowed to recover for 5 d before testing began. Mice were group housed 2–4 per cage.

During testing, access to water was restricted to 1 h per d. Licks were monitored during a 30-min session in which mice had free access to sucrose solution. Following experiments, mice were deeply anesthetized and perfused.

Brains were fixed in formalin, sliced at 80 μ m, and stained with thionin to visualize the extent of the lesions.

Behavior. Testing took place in a square behavioral chamber with a drinking spout located in the center of one wall. The spout was connected to a contact lickometer which recorded the time and duration of licks at 2,000 samples per s. Freely-behaving mice were allowed to voluntarily consume 10% (wt/vol) sucrose solution for ~30 min.

For electrophysiological recording experiments, mice were connected to a Blackrock Microsystems recording system before testing via a cable extending from the mouse's head to a motorized rotating commutator (Dragonfly), which allowed unimpeded movement.

All optogenetic experiments used bilateral illumination. Mice were connected to a 473-nm DPSS laser (Shanghai Laser) via fiber optic cables and placed inside the testing chamber⁴⁰. A rotating optical commutator (Doric) divided the beam (50:50) permitting bilateral stimulation and prevented the mice from becoming tangled. Optical stimulation was triggered by contact with the lickometer. Stimulation was either pulsed (10 mW; 3–100 Hz, 5-ms square pulse width, 1-s duration) or constant (10 mW; 1- or 2-s duration). A minimum delay of 5 s was imposed between stimulations. Stimulation parameters were consistent within a trial, but the order of stimulation was randomized between mice.

For optrode experiments, the experimental set up was the same as the previous experiments, except the mice were connected to both the laser and the recording system. Stimulation occurred in a blocked design in which mice had 1–4 blocks of trials (5–30 trials per block). Each session began with baseline trials in which no stimulation was presented and had at least two blocks (pseudo-randomized). For days in which two different frequencies were tested, the order of stimulation was randomized between mice. To test the efficacy of stimulation when mice were not licking, pulse trains were delivered in blocks of 12 trials (10-s inter trial interval) during free behavior. The stimulation frequency was held constant within a block but varied between blocks, and the order of stimulation was unique for each mouse.

Tracing. Wild-type mice (p60) were infected by 150 nl of EF-1 α promoter-driven Flex-AAV-GFP in the SNR (AP: 3.64; ML: 1.6; DV: 4.0). To visualize specific neurons in substantia nigra area that project to superior colliculus, 150 nl of rabies virus glycoprotein-coated Lenti-FuGB2-Cre (synapsin promoter)^{41,42} was injected into the superior colliculus (AP: 3.28; ML: 1.0; DV: 2.2). Two weeks after infection, brains were removed, postfixed overnight at 4 °C, and then cryoprotected with 30% sucrose in Tris-buffered saline (TBS). Brains were cut into 50- μ m coronal sections by cryostat (Leica CM 3000). Sections were treated with blocking solution (TBS containing 5% (vol/vol) normal goat serum and 0.2% (vol/vol) Triton X-100) for 2 h and incubated overnight at 4 °C with rabbit anti-tyrosine hydroxylase polyclonal antibody (1:1,000; Calbiochem, Cat. No. 657012) or guinea pig anti-VGAT polyclonal antibody (1:250; Synaptic Systems, Cat. No. 131 004). After washing three times for 10 min per wash with TBST (TBS containing 0.2% Triton X-100), sections were incubated with Alexa Fluor 555 IgG (1:500; Molecular Probes, Cat. No. A-21428) for 1 h at room temperature. Sections were counterstained with a 4',6-diamidino-2-phenylindole solution (DAPI; Sigma-Aldrich). After washing four times, the sections were coverslipped with FluorSave (CalBioChem) aqueous mounting medium. For axonal fiber tracing, images were taken by tile scan imaging using LSM 710 confocal microscope (Zeiss) with a 10 \times objective under control of Zen software (Zeiss). To verify the cell type (GFP-positive neurons) in substantia nigra, images were acquired by z-series (0.5- μ m intervals) using a 63 \times oil-immersion objective.

Muscimol inactivation. For muscimol inactivation experiments, wild-type mice ($n = 4$, 9 weeks old, all female) were implanted with bilateral cannulae targeting the lateral SC. Cannulae implantation and drug infusions were performed as previously described⁴³. Briefly, mice were anesthetized and steel cannulae (24 GA, 3-mm length below pedestal, Plastics One) were implanted at a 15° angle relative to the dorsoventral axis targeting the final coordinates, -3.5 AP, 1.85 ML and -1.8 DV (from dura). A stylet was inserted and protruded ~0.2 mm beyond the end of each cannula. Cannulae were secured in place with skull screws and dental acrylic. Mice were allowed to recover for one week before water restriction began. Mice were singly housed after surgery.

Thirsty mice were acclimated to the testing chamber and allowed to freely consume sucrose on the day before testing began. On test days, mice were lightly anesthetized with 1% isoflurane and the stylet was removed. Muscimol (1.0, 0.5, or 0.0 $\mu\text{g } \mu\text{l}^{-1}$ dissolved in PBS, order was randomized; Sigma) was infused at 0.1 $\mu\text{l min}^{-1}$ through custom made 31 GA steel injectors. Injectors were left in place for 2 min after infusions ended. Mice were allowed to recover in their home cage for 10 min before testing began. Tests were 30 min, during which licks were recorded as mice freely consumed sucrose solution.

Motion tracking. $\text{Vgat::ChR2}^{\text{SNR} \rightarrow \text{SC}}$ mice ($n = 7$) and a subset of $\text{Vgat::eYFP}^{\text{SNR} \rightarrow \text{SC}}$ mice ($n = 4$) that were used during licking experiments were used for motion analysis. Mice were connected to the laser as described above and placed on an elevated platform (14 \times 22.9 cm rectangle, elevated 33.7 cm), which was enclosed on only one side to allow for visibility for motion capture. The three-dimensional location of a 6.35-mm diameter reflective spherical marker placed on the head was recorded at 100 frames per s using eight infrared motion tracking cameras (Motion Analysis) placed around the platform. The location of the reflective marker was captured in millimeters relative to an x, y, z coordinate origin.

Stimulation trials were conducted in blocks of 10–12, each block consisting of a single stimulation parameter, with the order of these blocks randomized between mice. Stimulation occurred during free behavior, when the mouse was displaying a neutral posture, with a minimum inter-trial interval of 10 s. Stimulation was a 1-s pulse train, with the frequency varying between conditions (3, 10, 50, 100 or laser continuously on), and with a pulse width of 5 ms. Laser, motion capture and lever press data sets were aligned using TTL timestamps in the Cerebus data acquisition system (Blackrock Microsystems). Head speed in three-dimensional space was calculated from the raw x, y, z position data generated in Cortex (Motion Analysis) during motion capture.

Headfixed optogenetic stimulation. Vgat-Cre mice ($n = 5$; 3 male; 9–12 weeks old) were injected with ChR2 in the SNR and implanted with optic fibers targeting the lateral SC as described above. Three male Vgat-Cre mice implanted with optic fibers served as controls. In addition to optic fibers, a headpost situated along the medial-lateral axis was also cemented to the skull to allow mice to be headfixed. Mice were singly housed after surgery.

Each mouse was kept in an elevated plastic tunnel (inner diameter: 41 mm), with its head reaching out and being fixed by two stabilized clamps holding side-bars of the headpost. Heights of the tunnel and clamps were aligned before each session to ensure the comfort of mice. A steel tube (inner diameter: 1 mm) was placed directly in front of the mouse. We delivered 10% sucrose through the tube at a constant speed of 0.5 ml min^{-1} , controlled by the speed clamp on the tubing. Optical stimulation was triggered by an initial contact to the water-delivering tube in the same manner to experiments described above. Each session lasted 30 min and optical stimulation parameter remained constant throughout a session. The order of stimulation was randomized between mice. Mice were trained on the headfixed set up for one session before testing began.

To test whether optical stimulation of nigroreticular projections affected whisking or blinking, mice were head-fixed, and rested on a platform directly in front of a video camera, which recorded video of the frontal view during the experimental session. Optic stimulation was triggered manually via LabView laser control software. Each stimulation condition consisted of 40 trials with an inter-trial interval of 3 s. The order of stimulation parameters is randomized across mice. Whisking and blinking were manually scored in slow motion from the videos by two independent observers.

Histology. Following completion of experiments, mice were deeply anesthetized with isoflurane and perfused with 4% paraformaldehyde. Brains were post fixed in paraformaldehyde for ~24 h and then transferred to sucrose. For electrophysiology experiments, brains were sliced at 100 μm and stained with thionin. For optogenetics experiments, brains were sliced at 60 μm with a Vibratome. Slices were incubated with primary chicken anti-GFP (1:1,000, AbCam, Cat. No. ab13970) and Vgat primary rabbit anti- Vgat (1:1,000, Millipore, Cat. No. ab5062P) with 10% goat serum and 0.25% Triton X-100 overnight at 4 °C. Secondary antibodies (Alexa Fluor 594 (Cat. No. A-11037) goat anti-rabbit and Alexa Fluor 488 goat anti-chicken (Cat. No. A-11039)) were used to visualize

Vgat and GFP, respectively (1:250, Molecular Probes). Images were acquired with a Zeiss Axio Zoom.V16. The locations of electrodes, fibers and injections were compared with the atlas of Paxinos and Franklin⁴⁴.

Fluorescence quantification. To quantify ChR2-eYFP fluorescence intensity, a single image of a coronal brain section was acquired for each mouse (Zeiss Axio Zoom.V16). Identically sized regions of interest were drawn within the SNR, lateral SC, and medial SC of each hemisphere. The average pixel intensity for each region of interest was taken. Values were normalized to the background fluorescence (equally sized ROI from hippocampus of the same hemisphere in the same image).

Analysis. Motion tracking and headfixed behavior scoring were performed by researchers blinded to group identity. All other data collection and analysis were not performed blind to the conditions of the experiments. No animals or data points have been excluded.

Bout analysis was used to determine lick bouts. Based on previous analysis of rodent licking¹⁷, we defined the start of a bout as 3 or more licks occurring at >3 Hz and being preceded by at least 1 s in which no licks were recorded. The end of the bout was defined as the last lick that was followed by at least 1 s in which no licks were recorded. Neurons were considered to increase or decrease activity during the initiation of a bout if the spike rate within 500 ms on each side of the first lick within a bout was significantly different from the baseline period 1,500–500 ms before the start of a bout (paired t test, $P < 0.05$).

To examine the relationship between licking and single-unit spike rate, the lick rate and instantaneous spike rate within a bout of licks were sampled in 10-ms bins and Pearson correlation was then performed on the binned rates. To determine the phase relationship between the lick cycle and the neural oscillations, the maximum and minimum firing rates within the lick cycle were calculated. The data were transformed to polar coordinates such that 0 degrees represents the time of tongue contact with the spout. For optrode experiments, a neuron was determined to be light responsive if its firing rate was reduced during the stimulation epoch relative to the firing rate during same amount of time immediately preceding stimulation (paired t test, $P < 0.05$).

The probability that $\text{Vgat::ChR2}^{\text{SNR} \rightarrow \text{SC}}$ stimulation would cause an extended pause in licking was calculated for early (first ten trials) and late (last ten trials) epochs. A pause was defined as no licks occurring within 500 ms of the termination of stimulation.

Statistics. Data were analyzed using Matlab and Graphpad Prism. Data were assumed to be normal, but this was not formally tested. Corrections for multiple comparisons were performed where appropriate. All statistical tests were two-sided. No statistical methods were used to predetermine sample sizes.

Code availability. Matlab and Labview codes for controlling the laser and triggering stimulation when mice contact lick spout are available on request.

A **Supplementary Methods Checklist** is available.

36. Vong, L. *et al.* Leptin action on GABAergic neurons prevents obesity and reduces inhibitory tone to POMC neurons. *Neuron* **71**, 142–154 (2011).
37. Sparta, D.R. *et al.* Construction of implantable optical fibers for long-term optogenetic manipulation of neural circuits. *Nat. Protoc.* **7**, 12–23 (2012).
38. Faingold, C.L. & Randall, M.E. Neurons in the deep layers of superior colliculus play a critical role in the neuronal network for audiogenic seizures: mechanisms for production of wild running behavior. *Brain Res.* **815**, 250–258 (1999).
39. Faingold, C. & Casebeer, D. Modulation of the audiogenic seizure network by noradrenergic and glutamatergic receptors of the deep layers of superior colliculus. *Brain Res.* **821**, 392–399 (1999).
40. Rossi, M.A., Sukharnikova, T., Hayrapetyan, V.Y., Yang, L. & Yin, H.H. Operant self-stimulation of dopamine neurons in the substantia nigra. *PLoS One* **8**, e65799 (2013).
41. Kato, S. *et al.* A lentiviral strategy for highly efficient retrograde gene transfer by pseudotyping with fusion envelope glycoprotein. *Hum. Gene Ther.* **22**, 197–206 (2011).
42. Nelson, A. *et al.* A circuit for motor cortical modulation of auditory cortical activity. *J. Neurosci.* **33**, 14342–14353 (2013).
43. Rossi, M.A. *et al.* Prefrontal cortical mechanisms underlying delayed alternation in mice. *J. Neurophysiol.* **108**, 1211–1222 (2012).
44. Paxinos, G. & Franklin, K. *The Mouse Brain in Stereotaxic Coordinates* (Academic, 2003).